Environnement Canada
Centre météorologique canadien

Environment Canada
Canadian Meteorological Centre

Processing of

hyperspectral infrared sounder radiances

(AIRS, CrIS and IASI instruments)

at the Canadian Meteorological Centre

Version 1.3

June 2016

Revision history			
Version	Date	Author/modifications	Remarks
1.0 (AIRS)	2007/10/01	A. Beaulne, N. Wagneur	Initial document for AIRS
1.0 (IASI)	2011/04/08	S. Heilliette	Initial document for IASI
1.1 (AIRS)	2011/04/08	A. Beaulne, S. Heilliette	Modifications for GDPS “Strato2b”
1.1 (IASI)	2014/04/30	A. Beaulne	Addition of IASI Metop-1
1.2	2015/06/15	A. Beaulne, S. Heilliette	-Modifications for GDPS 4.0.0 -Merging of the AIRS and IASI doc
1.3	2016/06/06	A. Beaulne, S. Heilliette	-Modifications for GDPS 5.0.0 -Addition of CrIS

Table of Contents

1. Introduction. ______ 4

2. Flowchart of radiance processing. ______ 5

3. Observed radiance. ______ 7

4. Simulated radiance. ______ 7

5. Channels used in data assimilation. ______ 8

6. Bias correction. ______ 13

7. Quality control. ______ 14

8. Horizontal thinning. ______ 18

9. Monitoring. ______ 19

10. References. ______ 26

11. Glossary. ______ 27

Appendix A. BURP descriptors for hyperspectral infrared sounders (based on BUFR). 28

1. Introduction.

This document is a summary description of the operational processing of the hyperspectral infrared sounders radiances at the Canadian Meteorological Centre (CMC). An overview of the radiances, bias correction, quality control, data thinning and operational monitoring is presented. The current revision of this document covers the assimilation of the AIRS, CrIS and IASI data within the GDPS 5.0.0 implementation of December 2015.

The following table summarizes all implementations related to these instruments.

GDPS version	**Date**	**Description**
?	2008/05/28	- Addition of the AIRS instrument from satellite AQUA, assimilation of 87 channels with removal of the four highest-peaking in the Polar Regions (30 degrees from the poles). - Thinning at 250km. - Bias correction using BT predictor.
2.2.0	2011/11/16	- Addition of the IASI instrument from satellite Metop-1(B), assimilation of 62 channels. - With the model lid now at 0.1hPa, removal of the restrictions near the poles for AIRS. - Thinning at 150km.
3.1.1	2014/05/06	- Addition of the IASI instrument from satellite Metop-2(A), assimilation of 62 channels.
4.0.0	2014/11/18	- Assimilation of 142 channels for both AIRS and IASI instruments. - Bias correction using three geopotential thickness predictors.
5.0.0	2015/12/15	- Addition of the CrIS instrument from satellite NPP, assimilation of 103 channels.

The number of individual data elements assimilated from hyperspectral infrared sounders now exceeds 7 millions per day which is more than half the total number of data elements coming from all sources (conventional and radiances) which is now over 12 millions per day.

This document is organised in the following way. First, a flowchart in section 2 gives a summary of the different steps in the processing of the radiances. In sections 3 through 8, each process is described individually. In the final section, a description of the monitoring is presented.

2. Flowchart of radiance processing.

The different steps leading to the assimilation of hyperspectral radiances are illustrated in the following flowchart, which has been modified since the use of the Maestro sequencer in November 2014. A gray wavy bottom edge rectangle represents a BURP file while a blue rounded corners rectangle is a process. Variables shown are the observed radiance (O), the bias corrected radiance (O'), the trial simulated radiance (P) and the analysis simulated radiance (A). The processes are:

1) Start with a DERIALT file,
2) From file in (1), compute the radiance bias correction (O'-O), using the bias correction coefficient file, and apply to raw observed radiance (O) to obtain the corrected radiance (O'),
3) From file in (2), compute the innovation (O'-P) and perform quality control including channel selection, all using the EnVar, creating the EVALALT file,
4) From file in (3), apply a thinning at 150km, creating the BGCKALT file,
5) [not shown] Also from file in (3), compute the innovation (O'-A) using only the conventional type of data in a 3Dvar analysis (Gauthier et al., 1999) and, from the resulting file, apply a quality control and then a thinning at 200km,
6) [not shown] From file in (5), create the bias correction table file and, using the historic from the last seven days, compute the coefficients and create the bias correction coefficient file to be used next date in step (2),
7) From file in (4), assimilation in the EnVar (Buehner et al., 2015).

The following flowchart processing is executed in distinct tasks for AIRS, CriS and IASI radiances, since they are considered independent observation families. We will use ${instr} in the flowchart to refer to either of these instruments.

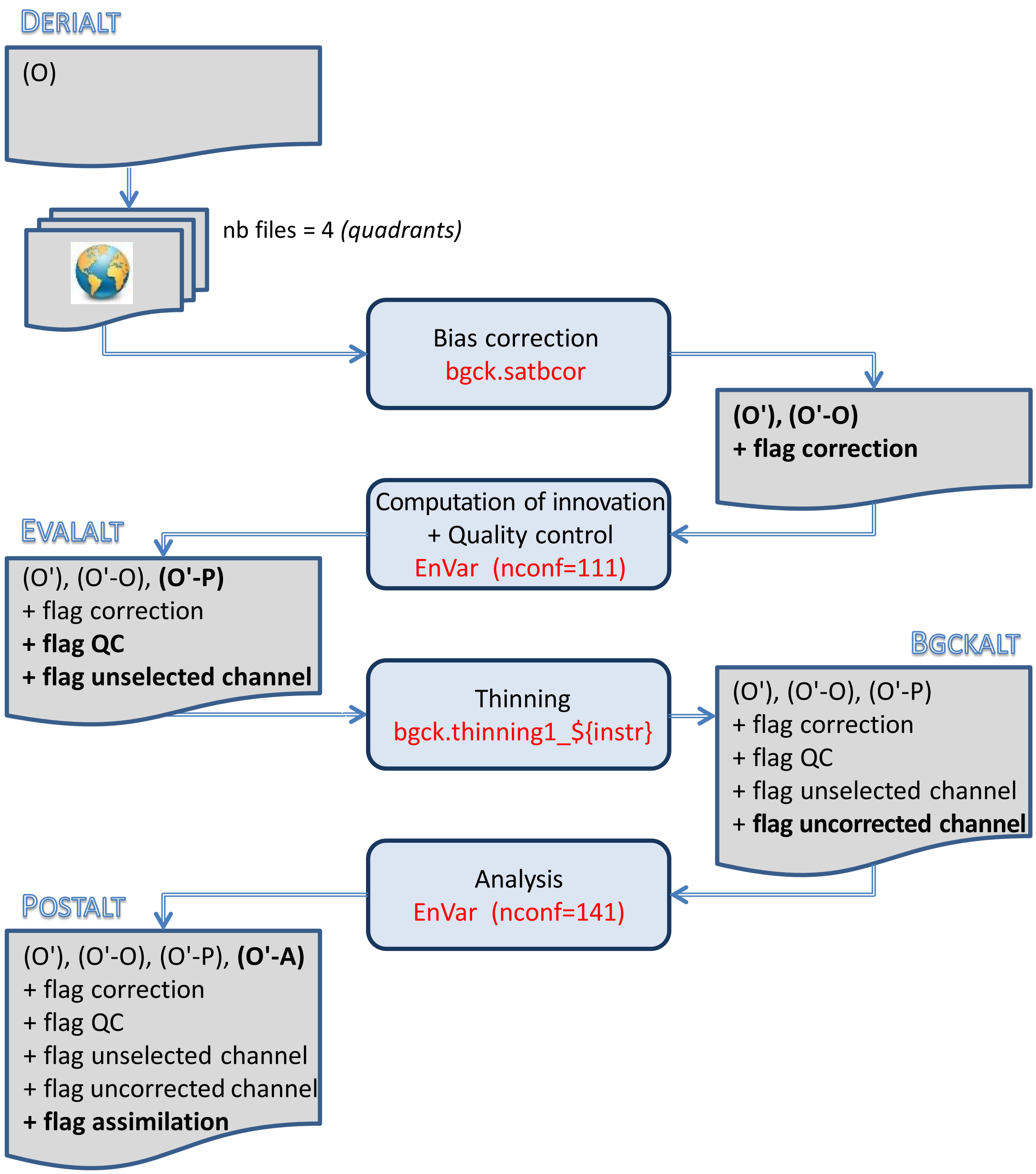

Figure 1. Processing of AIRS, CrIS or IASI radiances.

3. Observed radiance.

Hyperspectral observations come from the following sources:

- The AIRS instrument onboard the AQUA satellite
- The CrIS instrument onboard the NPP satellite
- The IASI instrument onboard Metop-1(B) and Metop-2(A) satellites.

and are received as BUFR files from an operational NESDIS server in Washington DC. The AAPP (ATOVS and AVHRR Pre-processing Package) software has already processed the observations for some quality control, navigation and calibration functions. The BUFR files are collected over time and merged to create data files every 6 hours (at analysis times) which are then converted to CMC dbase and derivate (BURP) files. The derivate files are input for the pre-assimilation processing shown in Figure 1.

The AIRS instrument has 2378 infrared channels, with a resolution of approximately 13.5 km at nadir. CMC only receives a subset of 281 of these channels, and one out of nine profiles (the warmest in a AMSU-A footprint). The CrIS instrument has 1305 infrared channels, with a resolution of approximately 14 km at nadir. CMC receives all these channels, and one out of nine profiles (the central in an ATMS footprint). The IASI instrument has 8461 infrared channels, with a resolution of approximately 12 km at nadir. CMC only receives a subset of 616 of these channels, and one out of four profiles (the warmest in a AMSU-A footprint).

4. Simulated radiance.

In order to assimilate AIRS, CrIS or IASI radiances, we need to calculate the so-called (O-P) innovation $y-H(x)$, where:

y: observed (corrected) radiance (O),
x: model state (temperature TT, *natural log* specific humidity LQ,
surface pressure PS, surface temperature TS, surface winds UU and VV),
H: non-linear observation operator.
$H(x)$: simulated radiance (P)

Surface winds (UU,VV) are needed by the radiative transfer model to estimate surface emissivity over open water for the surface contribution.

The operator H includes the following:

- horizontal interpolation of the background model state (x) to instrument observation points;
- vertical interpolation of TT and LQ from the background hybrid levels to the RTTOV radiation model's pressure levels;
- computation of simulated instrument radiances using the RTTOV fast radiative transfer model.

The EnVar program used to assimilate data computes the innovations. Currently, we use the RTTOV-10 radiative transfer model, maintained and distributed by the EUMETSAT Satellite Application Facility on Numerical Weather Prediction (NWP SAF). The RTTOV web site can be found at: http://www.metoffice.com/research/interproj/nwpsaf/rtm/index.html.

5. Channels used in data assimilation.

The impressive quantity of channels found on hyperspectral infrared sounders provides very accurate data about the atmosphere to support weather forecasting and allows retrievals of the concentrations of various trace gases. These instruments cover the spectral range from 645 to 2760 cm^{-1} (3.6 to 15.5 um) at very high resolution.

A typical radiance spectrum can be seen in Figure 2, computed here for IASI using a standard midlatitude profile (Han and McNally, 2010). This very detailed spectrum can be interpreted as composed of broad bands and regions that are of particular interest. Table 1 (adapted from Blumstein et al., 2004) shows the various usage of these main spectral ranges in which were added the number of channels from each of the instruments we currently assimilate in our systems. Finally, Tables 2 to 4 give the spectroscopic information on each of these channels.

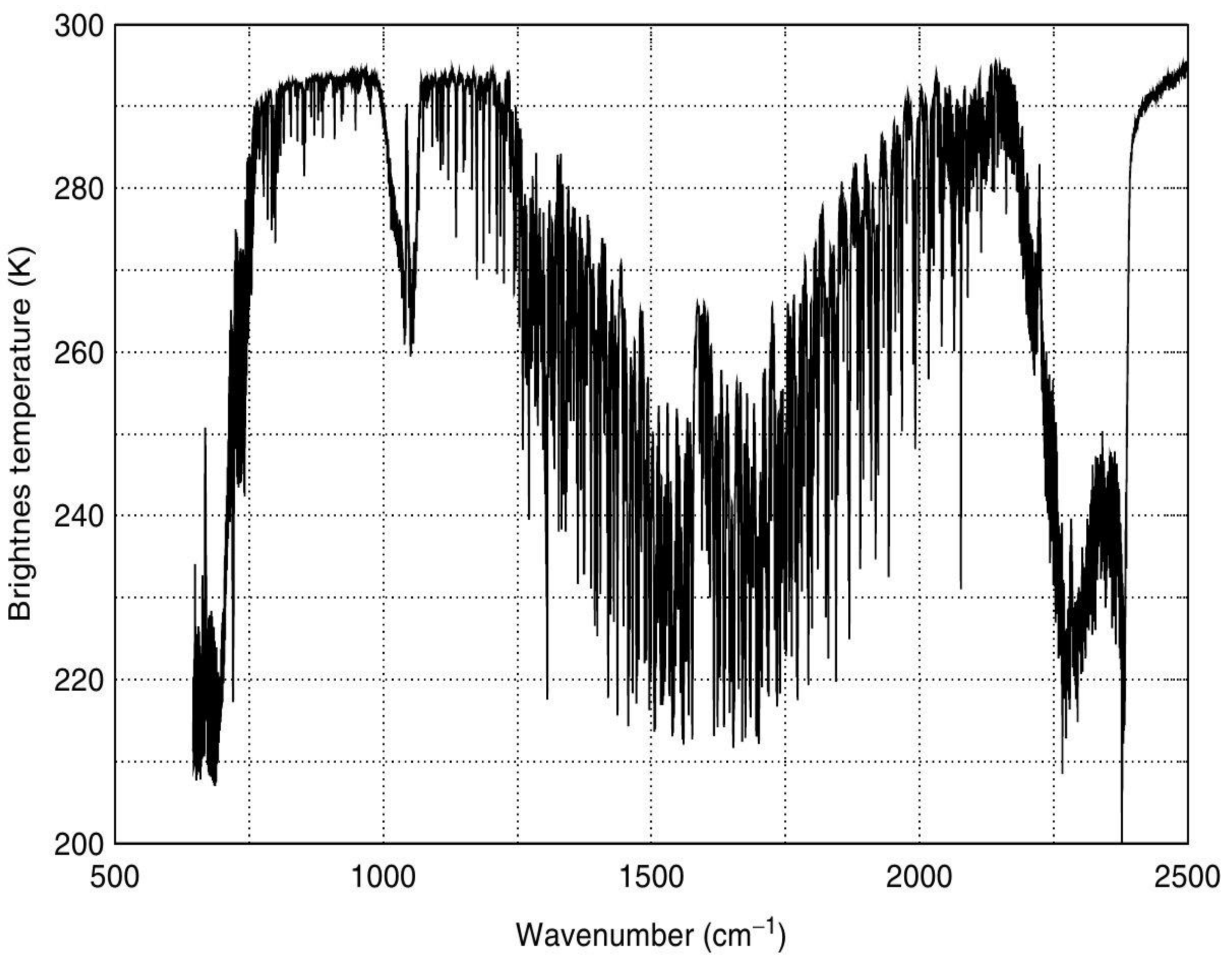

Figure 2. The IASI IR spectrum computed from a standard midlatitude profile (Han and McNally, 2010).

Band	Region	Spectral Region (cm^{-1})	Usage	Absorption band	AIRS (142 ch)	CrIS (103 ch)	IASI (142 ch)
B1	R1	650 – 770	Temperature profile	CO_2	62	44	75
		770 – 790	Temperature profile	CO_2		2	6
B1	R2	790 – 980	Surface and Cloud properties	Atmospheric Window	12	14	13
		980 – 1000	Surface and Cloud properties	Atmospheric Window		1	
B1	R3	1000 – 1070	Ozone sounding	O_3			
		1070 – 1080	Surface and Cloud properties	Atmospheric Window	2		
B1	R4	1080 – 1150	Surface and Cloud properties	Atmospheric Window	2		1
		1150 – 1210	Surface and Cloud properties	Atmospheric Window			3
B2	R5	1210 – 1650	Humidity profile; CH_4 and N_2O properties	H_2O	36	27	32
		1650 – 2100	Humidity profile	H_2O		2	3
B3	R6	2100 – 2150	CO column amount	CO			
B3	R7	2150 – 2250	Temperature profile N_2O column amount	CO_2 and N_2O	13	6	9
B3	R8	2350 – 2420	Temperature profile	CO_2	15	6	
B3	R9	2420 – 2700	Surface and Cloud properties	Atmospheric Window		1	
B3	R10	2700-2760	CH_4 column amount	CH_4			

Table 1. Main spectral regions covered by hyperspectral infrared sounders (adapted from Blumstein and al., 2004), their use and the number of channels we currently assimilate in them. The gray areas have been added and were not spectral regions identified in their article.

Channel number	Central wavenumber (cm $^{-1}$)	Wavelength (μm)	Channel number	Central wavenumber (cm $^{-1}$)	Wavelength (μm)	Channel number	Central wavenumber (cm $^{-1}$)	Wavelength (μm)
69	666.3	15.01	262	724.8	13.80	1708	1493.2	6.70
71	666.8	15.00	267	726.3	13.77	1723	1502.8	6.65
72	667.0	14.99	272	727.8	13.74	1740	1513.8	6.61
92	672.1	14.88	295	734.2	13.62	1748	1519.1	6.58
93	672.4	14.87	299	735.4	13.60	1756	1524.4	6.56
98	673.6	14.84	305	737.2	13.56	1771	1547.9	6.46
99	673.9	14.84	310	738.8	13.54	1777	1552.0	6.44
104	675.2	14.81	333	746.0	13.40	1783	1556.1	6.43
110	676.8	14.78	338	747.6	13.38	1794	1563.7	6.40
116	678.3	14.74	355	753.1	13.28	1800	1567.9	6.38
123	680.1	14.70	362	755.3	13.24	1806	1572.1	6.36
128	681.5	14.67	375	759.6	13.17	1826	1586.3	6.30
129	681.7	14.67	475	801.1	12.48	1843	1598.5	6.26
138	689.5	14.50	484	804.4	12.43	1852	1605.0	6.23
139	689.8	14.50	497	809.2	12.36	1865	2181.5	4.58
144	691.1	14.47	528	820.8	12.18	1869	2185.1	4.58
145	691.4	14.46	587	843.9	11.85	1872	2187.8	4.57
150	692.8	14.44	672	871.3	11.48	1873	2188.8	4.57
151	693.0	14.43	787	917.3	10.90	1876	2191.5	4.56
156	694.4	14.40	791	918.7	10.88	1881	2196.1	4.55
157	694.7	14.40	843	937.9	10.66	1882	2197.0	4.55
162	696.1	14.37	870	948.2	10.55	1883	2197.9	4.55
168	697.7	14.33	914	965.4	10.36	1911	2223.9	4.50
169	698.0	14.33	950	979.1	10.21	1917	2229.6	4.49
172	698.8	14.31	1138	1072.5	9.32	1918	2230.5	4.48
173	699.1	14.30	1142	1074.4	9.31	1924	2236.2	4.47
174	699.4	14.30	1206	1106.8	9.04	1928	2240.0	4.46
175	699.7	14.29	1260	1135.5	8.81	2112	2391.1	4.18
179	700.8	14.27	1266	1218.5	8.21	2113	2392.1	4.18
180	701.1	14.26	1329	1251.4	7.99	2114	2393.0	4.18
185	702.5	14.24	1371	1285.5	7.78	2115	2394.0	4.18
186	702.7	14.23	1382	1291.7	7.74	2116	2395.0	4.18
190	703.9	14.21	1424	1316.1	7.60	2117	2396.0	4.17
192	704.4	14.20	1449	1331.0	7.51	2118	2397.0	4.17
198	706.1	14.16	1455	1334.6	7.49	2119	2398.0	4.17
201	707.0	14.14	1466	1339.7	7.46	2120	2398.9	4.17
204	707.8	14.13	1477	1345.3	7.43	2121	2399.9	4.17
207	708.7	14.11	1500	1357.2	7.37	2122	2400.9	4.17
210	709.6	14.09	1519	1367.3	7.31	2123	2401.9	4.16
215	711.0	14.06	1538	1377.4	7.26	2128	2406.9	4.15
216	711.3	14.06	1545	1381.2	7.24	2134	2412.8	4.14
221	712.7	14.03	1565	1392.2	7.18	2141	2419.8	4.13
226	714.2	14.00	1574	1397.1	7.16			
227	714.5	14.00	1583	1402.2	7.13			
232	715.9	13.97	1593	1407.8	7.10			
252	721.8	13.85	1627	1427.2	7.01			
253	722.1	13.85	1636	1432.5	6.98			
256	723.0	13.83	1652	1441.9	6.94			
257	723.3	13.82	1669	1468.8	6.81			
261	724.5	13.80	1694	1484.4	6.74			

Table 2. AIRS channels used for assimilation.

Channel number	Central wavenumber (cm^{-1})	Wavelength (µm)	Channel number	Central wavenumber (cm^{-1})	Wavelength (µm)	Channel number	Central wavenumber (cm^{-1})	Wavelength (µm)
19	661.3	15.12	427	916.3	10.91	1250	2412.5	4.15
24	664.4	15.05	440	924.4	10.82	1252	2417.5	4.14
26	665.6	15.02	473	945.0	10.58	1254	2422.5	4.13
37	672.5	14.87	486	953.1	10.49			
39	673.8	14.84	496	959.4	10.42			
42	675.6	14.80	505	965.0	10.36			
44	676.9	14.77	514	970.6	10.30			
47	678.8	14.73	518	973.1	10.28			
49	680.0	14.71	520	974.4	10.26			
52	681.9	14.67	522	975.6	10.25			
54	683.1	14.64	534	983.1	10.17			
62	688.1	14.53	716	1212.5	8.25			
64	689.4	14.51	794	1310.0	7.63			
67	691.3	14.47	796	1312.5	7.62			
72	694.4	14.40	798	1315.0	7.60			
75	696.3	14.36	814	1335.0	7.49			
80	699.4	14.30	836	1362.5	7.34			
85	702.5	14.23	840	1367.5	7.31			
87	703.8	14.21	842	1370.0	7.30			
90	705.6	14.17	844	1372.5	7.29			
97	710.0	14.08	847	1376.3	7.27			
99	711.3	14.06	850	1380.0	7.25			
102	713.1	14.02	853	1383.8	7.23			
110	718.1	13.93	856	1387.5	7.21			
112	719.4	13.90	865	1398.8	7.15			
116	721.9	13.85	867	1401.3	7.14			
124	726.9	13.76	871	1406.3	7.11			
130	730.6	13.69	874	1410.0	7.09			
132	731.9	13.66	879	1416.3	7.06			
134	733.1	13.64	886	1425.0	7.02			
136	734.4	13.62	889	1428.8	7.00			
143	738.8	13.54	900	1442.5	6.93			
148	741.9	13.48	924	1472.5	6.79			
151	743.8	13.45	927	1476.3	6.77			
153	745.0	13.42	945	1498.8	6.67			
156	746.9	13.39	991	1556.3	6.43			
158	748.1	13.37	994	1560.0	6.41			
160	749.4	13.34	1007	1576.3	6.34			
164	751.9	13.30	1094	1685.0	5.93			
167	753.8	13.27	1132	1732.5	5.77			
169	755.0	13.25	1169	2210.0	4.52			
175	758.8	13.18	1173	2220.0	4.50			
186	765.6	13.06	1175	2225.0	4.49			
189	767.5	13.03	1177	2230.0	4.48			
200	774.4	12.91	1179	2235.0	4.47			
216	784.4	12.75	1185	2250.0	4.44			
228	791.9	12.63	1241	2390.0	4.18			
239	798.8	12.52	1243	2395.0	4.18			
255	808.8	12.36	1245	2400.0	4.17			
275	821.3	12.18	1248	2407.5	4.15			

Table 3. CrIS channels used for assimilation.

Channel number	Central wavenumber (cm $^{-1}$)	Wavelength (µm)	Channel number	Central wavenumber (cm $^{-1}$)	Wavelength (µm)	Channel number	Central wavenumber (cm $^{-1}$)	Wavelength (µm)
32	652.8	15.32	335	728.5	13.73	2907	1371.5	7.29
38	654.3	15.28	347	731.5	13.67	2944	1380.8	7.24
44	655.8	15.25	350	732.3	13.66	2951	1382.5	7.23
50	657.3	15.21	354	733.3	13.64	2977	1389.0	7.20
57	659.0	15.17	356	733.8	13.63	2990	1392.3	7.18
63	660.5	15.14	360	734.8	13.61	2993	1393.0	7.18
76	663.8	15.07	366	736.3	13.58	3008	1396.8	7.16
79	664.5	15.05	371	737.5	13.56	3027	1401.5	7.14
82	665.3	15.03	373	738.0	13.55	3030	1402.3	7.13
87	666.5	15.00	375	738.5	13.54	3049	1407.0	7.11
104	670.8	14.91	377	739.0	13.53	3058	1409.3	7.10
109	672.0	14.88	379	739.5	13.52	3087	1416.5	7.06
116	673.8	14.84	381	740.0	13.51	3107	1421.5	7.03
122	675.3	14.81	389	742.0	13.48	3110	1422.3	7.03
128	676.8	14.78	404	745.8	13.41	3127	1426.5	7.01
135	678.5	14.74	407	746.5	13.40	3151	1432.5	6.98
141	680.0	14.71	410	747.3	13.38	3160	1434.8	6.97
154	683.3	14.64	414	748.3	13.36	3228	1451.8	6.89
160	684.8	14.60	416	748.8	13.36	3263	1460.5	6.85
167	686.5	14.57	426	751.3	13.31	3303	1470.5	6.80
173	688.0	14.53	428	751.8	13.30	3432	1502.8	6.65
180	689.8	14.50	432	752.8	13.28	3467	1511.5	6.62
185	691.0	14.47	434	753.3	13.28	3497	1519.0	6.58
199	694.5	14.40	445	756.0	13.23	3499	1519.5	6.58
205	696.0	14.37	457	759.0	13.18	3518	1524.3	6.56
212	697.8	14.33	515	773.5	12.93	3610	1547.3	6.46
213	698.0	14.33	546	781.3	12.80	3646	1556.3	6.43
214	698.3	14.32	552	782.8	12.78	3673	1563.0	6.40
217	699.0	14.31	566	786.3	12.72	3710	1572.3	6.36
219	699.5	14.30	571	787.5	12.70	3763	1585.5	6.31
224	700.8	14.27	573	788.0	12.69	4920	1874.8	5.33
226	701.3	14.26	646	806.3	12.40	4991	1892.5	5.28
230	702.3	14.24	662	810.3	12.34	5371	1987.5	5.03
232	702.8	14.23	668	811.8	12.32	6135	2178.5	4.59
236	703.8	14.21	756	833.8	11.99	6149	2182.0	4.58
239	704.5	14.19	867	861.5	11.61	6158	2184.3	4.58
243	705.5	14.17	921	875.0	11.43	6161	2185.0	4.58
246	706.3	14.16	1027	901.5	11.09	6174	2188.3	4.57
249	707.0	14.14	1046	906.3	11.03	6205	2196.0	4.55
252	707.8	14.13	1121	925.0	10.81	6209	2197.0	4.55
262	710.3	14.08	1133	928.0	10.78	6213	2198.0	4.55
265	711.0	14.06	1191	942.5	10.61	6317	2224.0	4.50
269	712.0	14.04	1194	943.3	10.60			
275	713.5	14.02	1271	962.5	10.39			
282	715.3	13.98	2019	1149.5	8.70			
299	719.5	13.90	2094	1168.3	8.56			
300	719.8	13.89	2119	1174.5	8.51			
323	725.5	13.78	2213	1198.0	8.35			
327	726.5	13.76	2321	1225.0	8.16			
329	727.0	13.76	2398	1244.3	8.04			

Table 4. IASI channels used for assimilation.

6. Bias correction.

Radiance observations, as well as radiative transfer models, contain important errors. It is essential to remove the radiance biases in order to optimally extract the information content for data assimilation. Radiance biases are evaluated using an “unbiased” 3DVar analysis (A) without any satellite radiances assimilated.

Radiance < *O-A* > biases (< > indicates time average) manifest in two different ways, one of which depends on a global bias and the second of which is air-mass dependent. This led to a two-step approach at CMC, the first of which is to remove the global bias, followed by a second step that removes the remaining bias, using a linear regression between the bias and the following model predictors:

- geopotential thickness of the layer 1000hPa-300hPa (T1);
- geopotential thickness of the layer 200hPa-50hPa (T2);
- geopotential thickness of the layer 50hPa -5hPa (T3);
- view angle (SV)   [Cris only]

The view angle predictor is expected to be included for AIRS and IASI on a further implementation.

A different set of regression coefficients are computed for each satellite, instrument and channel. The regression coefficients are recomputed every 6 hours, based on the O-A/predictor statistics of the previous 7 days.

The implementation of this radiance correction at the level of the BURP observation file proceeds in the following way:

1) a data quality flag indicates that a radiance has been corrected (bit 6 is set);
2) the bias correction itself appears as a separate element in the BURP file.

Therefore, it is always possible to re-construct the original observed radiance by using the corrected radiance and its correction. Appendix A has a summary of the main BURP descriptors associated with the various hyperspectral data.

7. Quality control

This step consists in running the EnVar (current operational revision 690, tags v_2.1.2) in innovation mode. In addition to compute the radiance O-P and to create the corresponding block in each records of the output file, the complete quality control of AIRS, CrIS and IASI observations will be performed since it is built in for these families in the EnVar (nconf = 111). As it goes through the process, each radiance datum will undergo a series of checks which could set various bits for different reasons, resulting in a final quality control flag that will be written in the output file (flag block : btyp = 15456, element = 212163). At the end, a radiance with a flag freed of these bits will be considered a suitable candidate for data assimilation until spatial thinning and EnVar analysis still remove data or further set some bits.

For informative and research purposes, results from various quality control internal computations (mainly related to cloud parameters) are also added to the output file (see Appendix A).

The different checks and resulting actions are explained in the following table. While the majority applies to all instruments, some applies only to a particular instrument when indicated.

<table>
<tr><th colspan="3">Radiance initial quality check</th></tr>
<tr><td>AIRS</td><td>Bit 2 [1]</td><td>set Bit 9</td></tr>
<tr><td>IASI</td><td>BURP element 033060 not zero and/or BURP element 033062 greater than 1</td><td>set Bit 9
(all channels in profile)</td></tr>
<tr><th colspan="3">Gross check
(on individual radiance)</th></tr>
<tr><td colspan="2">Observed or computed brightness temperature unrealistic : < 150 K or > 350 K</td><td>set Bit 9</td></tr>
<tr><th colspan="3">Determination of clear / cloudy profiles
(on observation profile)</th></tr>
<tr><th colspan="3">Preliminary guess</th></tr>
<tr><td colspan="2">Use of the Garand and Nadon (1998) algorithm</td><td>set Clear/Cloudy</td></tr>
<tr><th colspan="3">If clear, refinement to remove potential cloudy profiles</th></tr>
<tr><td>AIRS</td><td>Ancillary information about clouds
• Cloud fraction (BURP element 020010) > 5 %
• Sun zenith angle (BURP element 007025) < 90 (day)</td><td rowspan="2">set Cloudy</td></tr>
<tr><td>IASI</td><td>• Cloudy according to AVHRR radiance cluster analysis [2]</td></tr>
<tr><td colspan="2">Skin temperature difference threshold over water
• Water surface type (BURP element 008012 equal to 1)
• | Computed [3] minus guess skin temperature | over 1.5 deg K</td><td>set Cloudy</td></tr>
</table>

<table>
<tr><td colspan="2">Skin temperature difference threshold over land
• Land surface type (BURP element 008012 not equal to 1)
• | Computed [3] minus guess skin temperature | over 4.0 deg K</td><td>set Cloudy</td></tr>
<tr><td colspan="2">• Cloudy as determined by previous checks</td><td>set Bit 11 and 23
(all channels in profile)</td></tr>
<tr><td colspan="3">Determination of assimilation flag
(on individual radiance)</td></tr>
<tr><td colspan="3">Refinement to add potential clear radiance</td></tr>
<tr><td colspan="2">Insensitivity to clouds
• Bit 11
• Minimum height of jacobian sensitivity [4] sufficiently above consensus cloud top [5]</td><td>unset Bit 11 and 23</td></tr>
<tr><td colspan="3">If clear, refinement to remove unwanted radiance</td></tr>
<tr><td colspan="2">Rogue check
• Observed minus computed brightness temperature > 3 * observation error</td><td>set Bit 9 and 16</td></tr>
<tr><td>AIRS</td><td>Remove shortwave channels during day (Sun zenith angle < 100)
• Channel ≥ 1865</td><td rowspan="3">set Bit 11 and 7</td></tr>
<tr><td>CrIS</td><td>• Channel ≥ 1147</td></tr>
<tr><td>IASI</td><td>• Channel ≥ 5446</td></tr>
<tr><td colspan="2">Remove surface channels over land and over sea ice
• Land surface type (BURP element 008012 equal to 0) or
Sea-ice surface type (BURP element 008012 equal to 2)
• Minimum height of jacobian sensitivity [4] at surface or within 100mb of surface</td><td>set Bit 11 and 19</td></tr>
<tr><td colspan="2">Remove surface channels over water under conditions
• Water surface type (BURP element 008012 equal to 1)
• Minimum height of jacobian sensitivity [4] at surface or within 100mb of surface
• CERES water percentage (1 / 6 deg. resolution) < 0.99 or
CERES area averaged water percentage (2.5 deg. resolution) < 0.97 or
Presence of ice > 0.001 or
Albedo ≥ 0.17 or
Surface emissivity < 0.9</td><td>set Bit 11 and 19</td></tr>
<tr><td colspan="3">In all cases, refinement to remove unwanted radiance</td></tr>
<tr><td colspan="2">Remove channels with significant jacobian contribution above model top
• Not bit 9
• Transmittance at model top (0.1mb) < 0.95</td><td>set Bit 11 and 21</td></tr>
<tr><td colspan="2">Only keep channels which are used for assimilation (Section 5)
• Unselected (blacklisted)</td><td>set Bit 8</td></tr>
</table>

Notes on the quality control:

- A profile is not assimilated if data from the 2 windows channels (basic and alternate) are bad and/or if no channel pair is available for CO_2 slicing.

- CERES surface type (divided in 20 categories) and water fractions are read from a climatological file at 1/6 deg. resolution. Surface albedo (`NOMVAR='AL',IP1=60268832`) is read from the previous trials.glbhyb2 file (extension *_360m) while sea-ice (`NOMVAR='LG'`) and snow (`NOMVAR='SD',IP1=1195`) are read from the previous analyses.glbhyb2 file (extension *_000). Together, they allow for the refinement and determination of surface albedo, sea ice and snow surface type, water fraction (local and area averaged) and surface emissivity at profile locations.

[1] In the case of the AIRS instrument only, a radiance datum can already have its quality control flag (BURP element 212163) not zero (bit 2 set) at the Derialt step. This is done at the data decoding where BURP element 033032 is not zero.

[2] AVHRR (Advanced Very High Resolution Radiometer) is an imager with 2 visible/near IR channels (channels 1 at 0.6 μm and 2 at 1.0 μm), one shared channel (3a at day-time in the near IR at 1.6 μm, 3b at night-time in the thermal infrared at 3.7 μm) and 2 thermal infrared windows at 11 μm and 12 μm (channels 4 and 5). The pixel size is of approximately 1 km at nadir, and IASI field of views (FOVs) are co-registrated with AVHRRR pixels. Each IASI FOV contains approximately 100 AVHRR pixels. An automatic (unsupervised) classification algorithm is applied in AVHRR radiance space by EUMETSAT. As a result of this classification, the AVHRR pixels are separated into up to 6 classes. Each class is characterized by the fraction of the IASI FOV covered by the AVHRR pixels, the mean and the standard deviation of the radiance of each of the 6 AVHRR channels. This information is present in the level 1.c BUFR files (see Appendix A). As part of our IASI quality control, for each IASI FOV, and for each class the visible and near-IR mean and standard deviations of radiances are converted into albedos and the thermal IR mean and standard deviations of radiances into brightness temperatures to facilitate the physical interpretation of these parameters. Then, each class is subjected to a cloud detection algorithm. Firstly, the two tests applied to IASI radiances, i.e Garand-Nadon and the skin surface temperature difference test, are applied using the mean brightness temperatures of AVHRR channels 4 and 5. Additionally, during day time, an extra test is applied: the pixel is considered cloudy if the albedo of one of the visible and near IR channels 1, 2 and 3a exceeds a threshold (function of channel, surface type and observation geometry). For each IASI FOV, an "AVHRR pseudo cloud fraction" is calculated as the sum of the fraction of each cloudy AVHRR class. Also, for each IASI FOV, the "global standard deviation", computed combining all classes, is calculated for each AVHRR channel (visible, near-IR and thermal IR) as a measurement of FOV heterogeneity. An IASI FOV is considered cloudy according to AVHRR radiance cluster analysis if the AVHRR pseudo cloud fraction is greater than 5% or if the global standard deviation exceeds a threshold (channel, surface type and day/night dependent) for one AVHRR channel. Furthermore, for each cloudy class, a cloud effective height, based on the assumption of an overcast cloud covering the whole class, is calculated for AVHRR channels 4 and 5. This effective cloud height is always an underestimation of the real cloud height (in the sense that the real cloud is always higher than the effective overcast cloud). The consensus cloud top pressure, estimated by combining CO_2 slicing estimates, is therefore replaced by the cloud top pressure corresponding to the highest AVHRR effective height if this effective cloud is higher than the consensus effective cloud. The consensus cloud top pressure is used for the determination of channels unaffected by clouds.

[3] Computed skin temperatures are estimated using the observed radiances and by inversion of the radiative transfer equation assuming that temperature and humidity vertical profiles are perfect. It also assumes real guess skin temperatures over oceans and guess skin temperatures with hypothesis of unity emissivity over land.

[4] Starting at the surface, defined as the first level where *d Transmission / d log(Pressure)* gets over 0.01 of its maximum.

[5] The consensus is defined as the median cloud top from all CO_2-slicing solutions (between 1 and 13 possible values). If no solution found from CO_2-slicing, and not predetermined clear, cloud top is based on matching observed radiances (from a window channel) with the background radiance profile computed by RTTOV. The security margin (sufficiently above) is set to two times the standard deviation of the CO_2-slicing solutions, but cannot be below 50hPa.

8. Horizontal thinning.

In order not to overwhelm the assimilation system and to provide an appropriate volume of data for the analysis grid, the density of data from all satellites are reduced to a separation of about 150 km. This separation seems to be optimal with the current system, due to the fact that it assumes no horizontal correlation of the observational error for radiances and given the rather broad horizontal correlation functions of the background error.

The thinning process for hyperspectral infrared sounders data is summarized below. Remember that this process is done separately for AIRS, CrIS and IASI. A satellite radiance “profile” is defined here as radiance data from multiple channels at given location.

1) Data are separated into time slots, corresponding to each time step of the model background (trial) field. Currently, the time slot delta (dstepobs) is 15 minutes giving a total of 25 time slots in the 6-hour assimilation window.
2) For each time slot, data are grouped into 150 x 150 km square thinning boxes and filtered as described in steps (3) and (4) below.
3) Within each box, a priority scheme retains the profile which has the most assimilatable channels, as long as its distance from the center of the box is within 45km.
4) In the case more than one profile qualifies in step (3), the profile which is closest to the center of the box is chosen.

Profiles that are rejected by the thinning process are entirely removed from the output file. In addition, all radiance flags are checked for bias correction (bit 6). In the case it is unset, bit 11 is set (this is usually the case for blacklisted channels).

A thinning done at 200km resolution is also performed for the data which will be saved in the bias correction table files.

9. Monitoring.

The operational monitoring of hyperspectral infrared sounders radiances is part of the CMC on-line monitoring system, developed for all observations used in the EnVar assimilation. The address of this web site is the following:

Internal:

http://iweb.cmc.ec.gc.ca/~afsdwww/monitoring/index.html

External:

http://collaboration.cmc.ec.gc.ca/cmc/data_monitoring/

The external site requires a username and password for access that are easily available, by sending a request via e-mail to simon.pellerin@ec.gc.ca

The monitoring is divided in four parts:

- data reception;
- data quality monitoring;
- data included in the analysis;
- monthly means.

Information is available on the number of radiance data and their geographical distribution, both on reception and following data thinning. Time series of innovations are also available and their use is mainly to detect any drift in the satellite measurements and/or in the bias correction of the radiances. Maps of 6-hour innovations are available for each satellite, channel and synoptic hour, while monthly means of these are useful in detecting systematic errors in the system, if any should exist.

A few examples of monitoring plots are given in Figures 3 through 8. Figure 3 shows the geographical distribution of IASI profiles received at CMC (upper panel) and actually assimilated in the analysis after quality control and thinning (lower panel) for the global G2 run of June 16th, 2015 at 12Z. Time series of the volume of IASI profiles received (upper panel) and assimilated (lower panel) is presented in Figure 4 for each 6-hour global G2 run covering the 25-day time window prior to June 17th, 2015. Figure 5 (typically called dna-plots) shows in a two-dimensional convenient manner the standard deviation of the innovations O-P for each IASI Metop-2 suitable for assimilation channel (in the range 432 to 6317) for each 6-hour global G2 run covering the 25-day time window prior to June 17th, 2015. Complete information about innovations O-P, residuals O-A, brightness temperatures and number of profiles for a specific channel is available as presented in Figure 6 for IASI Metop-2 channel 3030 for each 6-hour global G2 run covering the 25-day time window prior to June 17th, 2015. For a specific channel, the values and geographical distribution of O-P can be shown for a specific global G2 run as in Figure 7 (upper panel) for IASI Metop-2 channel 3030 on June 16th, 2015 at 12Z, while monthly means are also available as shown in the lower panel for the month of May, 2015. Finally, Figure 8 shows a map distribution of the average 24-hour number of IASI profiles assimilated for the month of May, 2015, in cells of 10^o x 10^o.

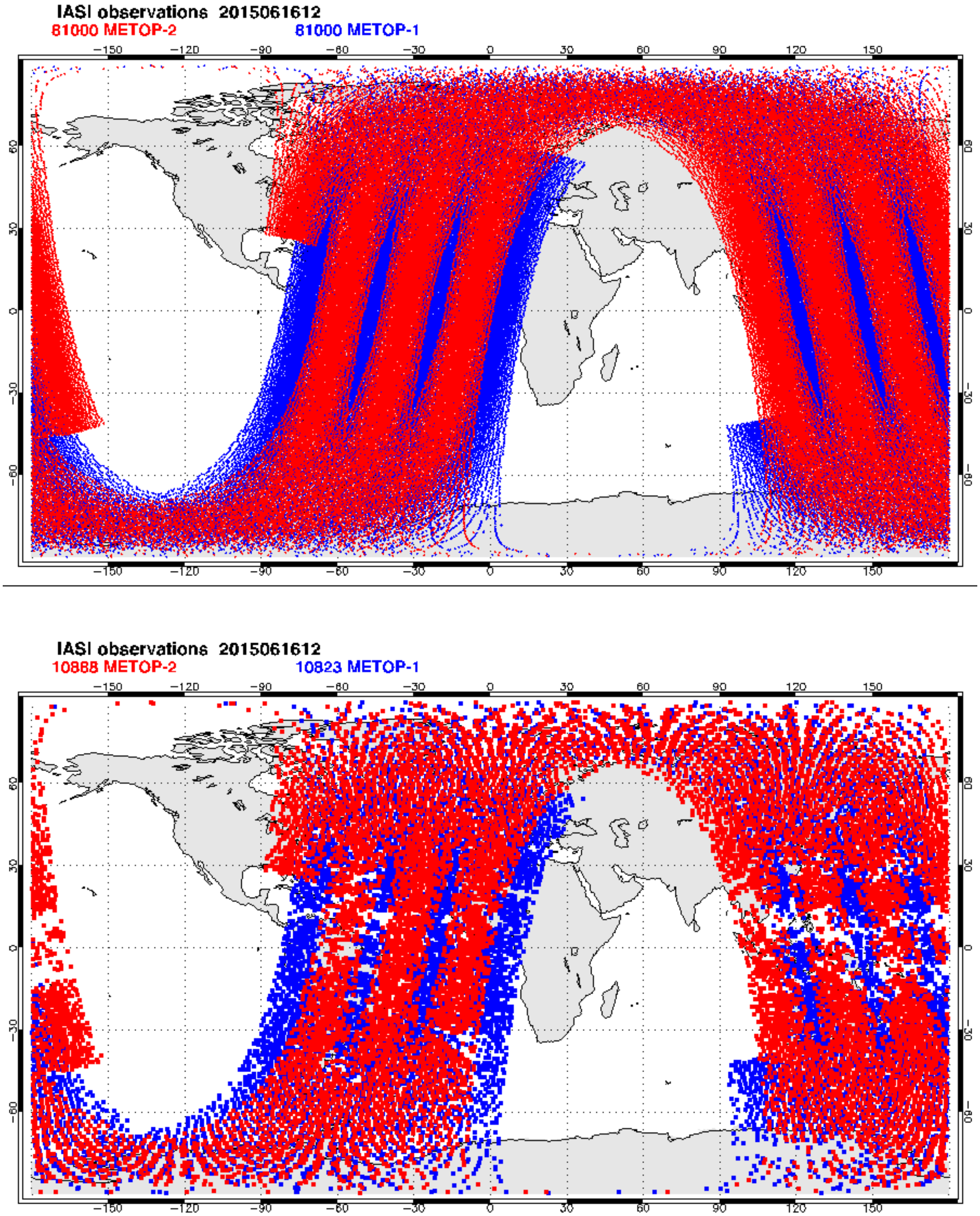

Figure 3. Distribution of IASI observation profiles received (upper panel) and included in the analysis (lower panel) for the operational EnVar global run G2 analysis of June 16th, 2015 at 12 UTC.

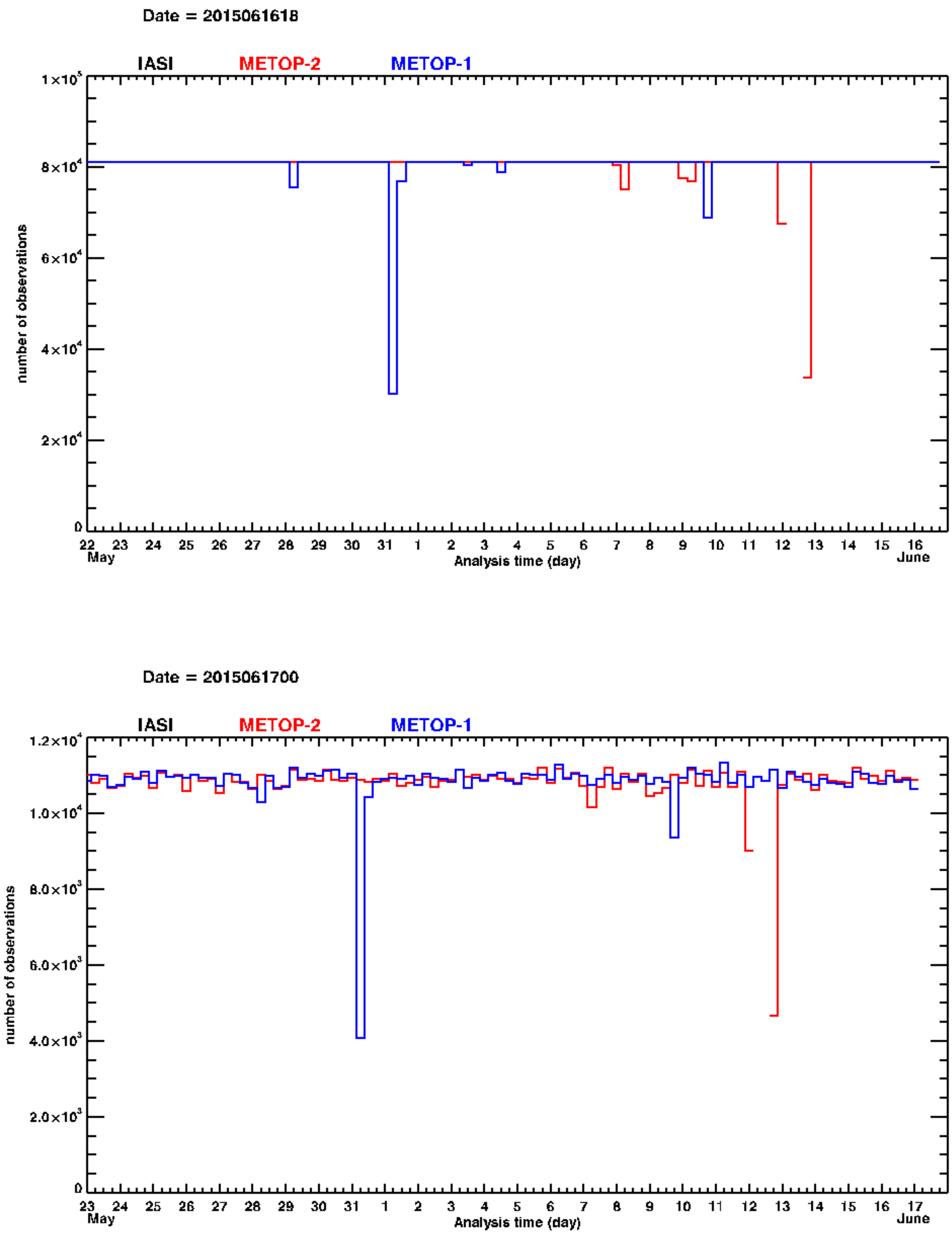

Figure 4. Time series of the number of IASI observation profiles received (upper panel) and included in the analysis (lower panel) for all operational EnVar global run G2 analysis of a 25-day time window prior to June 17th, 2015.

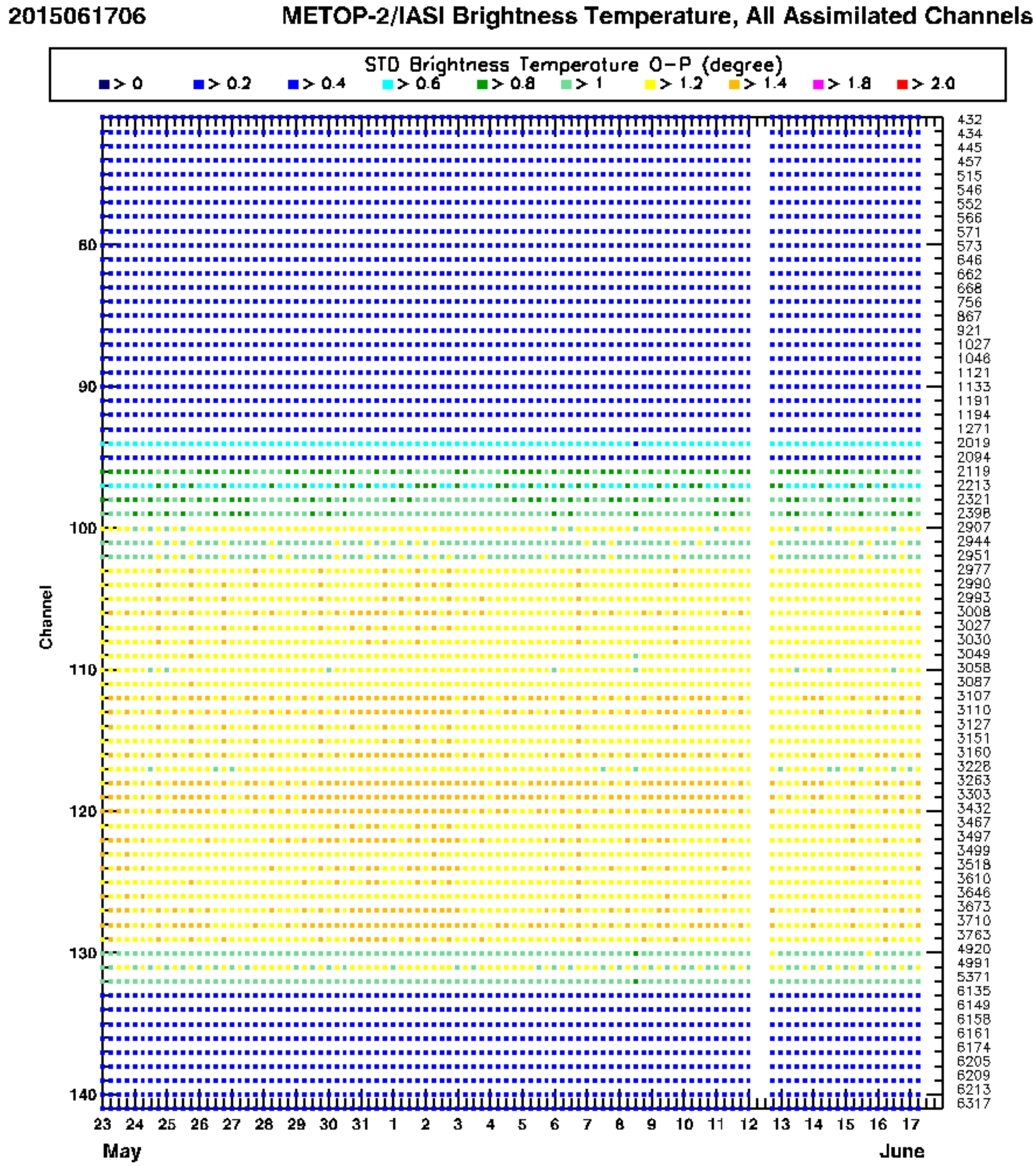

Figure 5. Time series of the innovation O-P standard deviation for IASI Metop-2 satellite and all channels suitable for assimilation in the range 432 to 6317, for all operational EnVar global run G2 analysis of a 25-day time window prior to June 17th, 2015.

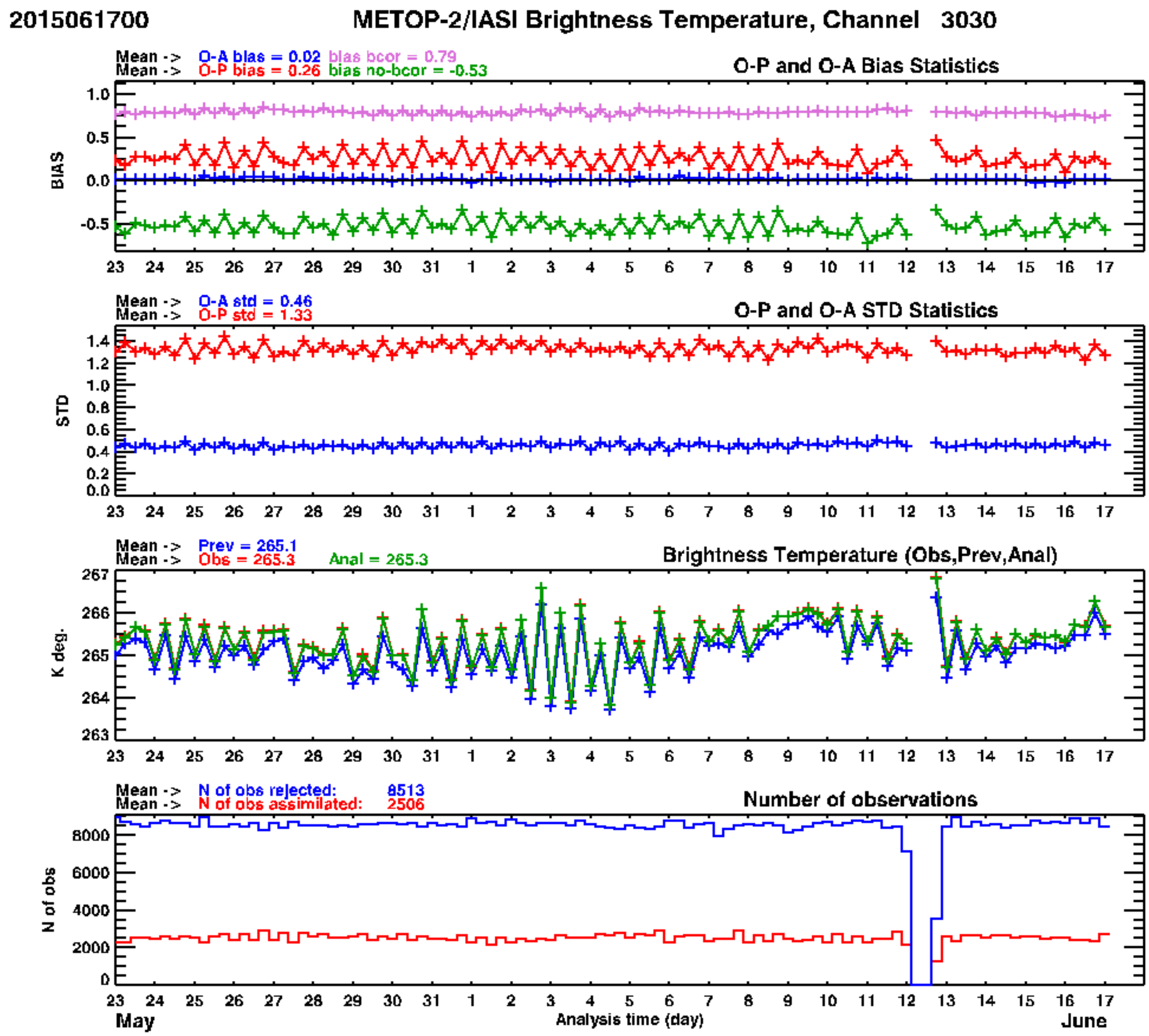

Figure 6. Time series of various statistics (bias, standard deviation, bias correction) for the innovations O-P and analysis residuals O-A and additional information for mean brightness temperatures (observations, trials, analysis) and number of assimilated/rejected profiles for IASI Metop-2 channel 3030, for all operational EnVar global run G2 analysis of a 25-day time window prior to June 17th, 2015.

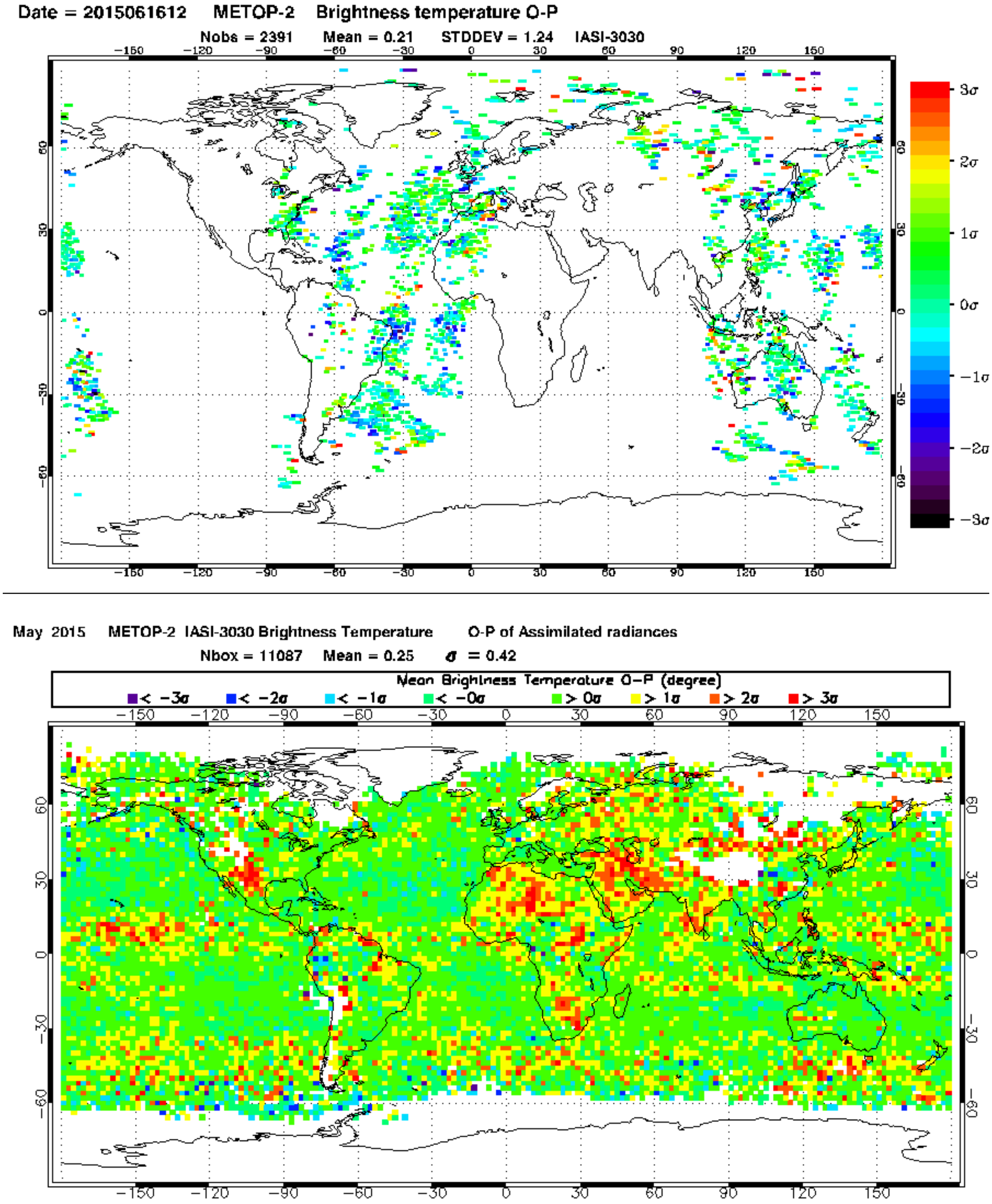

Figure 7. Upper panel : Distribution of IASI Metop-2 channel 3030 (O-P)/stddev values included in the analysis for the operational EnVar global run G2 analysis of June 16th, 2015 at 12 UTC. Lower panel : Monthly means of innovations O-P of assimilated radiances for IASI Metop-2 channel 3030 for May 2015, in 2° x 2° boxes.

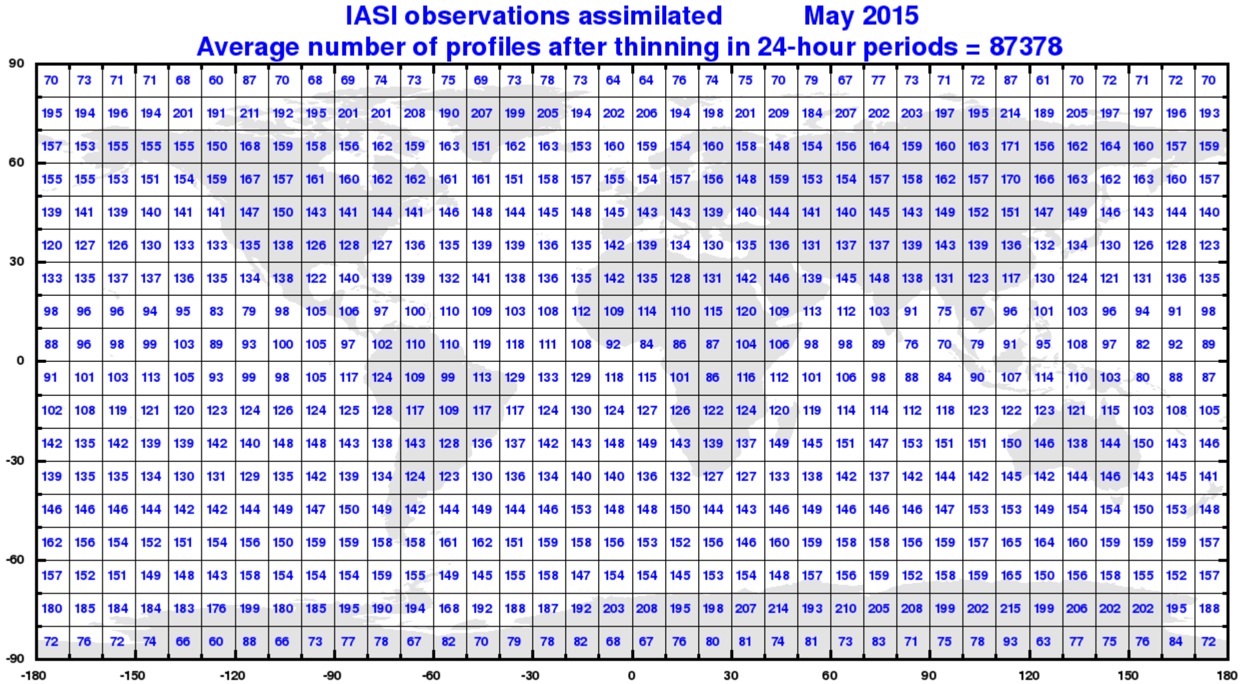

Figure 8. Monthly average of IASI number of observation profiles assimilated by the global EnVar system for G2 run in May 2015. In each 10^o x 10^o box, the plotted number indicates the average number within a 24-hour period.

10. References.

Buehner, M., R. McTaggart-Cowan, A. Beaulne, C. Charette, L. Garand, S. Heilliette, E. Lapalme, S. Laroche, S. R. Macpherson, J. Morneau and A. Zadra, 2015: Implementation of Deterministic Weather Forecasting Systems Based on Ensemble-Variational Data Assimilation at Environment Canada. Part I: The Global System. *Mon. Wea. Rev*., **143**, 2532-2559.

Blumstein, D., G. Chalon, T. Carlier, C. Buil, P. Hébert, T. Maciaszek, G. Ponce, T. Phulpin, B. Tournier, D. Siméoni, P. Astruc, A. Clauss, G. Kayal and R. Jegou, 2004: IASI instrument: technical overview and measured performances. *SPIE Proceedings*, **5543**, 196-207.

Garand, L., and S. Nadon, 1998: High-resolution satellite analysis and model evaluation of clouds and radiation over the Mackenzie basin using AVHRR data. *J. Climate*, **11**, 1976-1996.

Gauthier, P., C. Charette, L. Fillion, P. Koclas, and S. Laroche, 1999: Implementation of a 3D variational assimilation scheme at the Canadian Meteorological Center: Part I: The global analysis. *Atmos. Ocean*, **37,** 103-156.

Han, W. and A. P. McNally, 2010: The 4D-Var assimilation of ozone-sensitive infrared radiances measured by IASI. *Q. J. R. Meteorol. Soc.*, **136**, 2025-2037.

11. Glossary.

3DVar	3-Dimensional Variational [analysis]
AAPP	**ATOVS** and **AVHRR** Pre-processing Package
AIRS	Atmospheric Infrared Sounder
AQUA	[Latin word for “water”]
ATMS	Advanced Technology Microwave Sounder
ATOVS	Advanced **TIROS** Operational Vertical Sounder
AVHRR	Advanced Very High Resolution Radiometer
BUFR	Binary Universal Form for the Representation [of Meteorological Data]
BURP	Binary Universal Report Protocol
CERES	Clouds and the Earth’s Radiant Energy System
CMC	Canadian Meteorological Center
CrIS	Cross-track Infrared Sounder
EnVar	[Hybrid] Ensemble-Variational [analysis]
EUMETSAT	European Organization for the Exploitation of Meteorological Satellites
FOV	Field Of View
IASI	Infrared Atmospheric Sounding Interferometer
IR	Infrared
JMA	Japanese Meteorological Agency
Metop	Meteorological Operational [Satellite]
NESDIS	National Environmental Satellite, Data and Information Service
NPOESS	National Polar-Orbiting Operational Environmental Satellite System
NPP	**NPOESS** Preparatory Project
RTTOV	Radiative Transfer for **TOVS**
TIROS	Television and Infrared Observation Satellite

Appendix A.
BURP descriptors for hyperspectral infrared sounders (based on BUFR).

<u>NOTE</u>: BURP file code type is 183 for AIRS, 186 for IASI and 193 for CrIS.

Descriptor number	**Descriptor**
005042	Channel number
033032	Observation quality flag (AIRS)
033060	GQISFLAGQUAL quality flag (IASI)
033062	GQISQUALINDEXLOC quality flag (IASI)
025142	channel scaling factor (for IASI and AVHRR)
014046	Scaled IASI radiance
012163	Brightness temperature
012233	Brightness temperature correction
055043	Surface emissivity
007024	Satellite zenith angle
005021	Satellite azimuth angle
007025	Solar zenith angle
005022	Solar azimuth angle
008012	Land/sea qualifier
020010	Cloud fraction (AIRS and CrIS)
025085	Class fraction (see AVHRR radiance cluster analysis)
014047	Mean of scaled AVHRR radiance
014048	Standard deviation of scaled AVHRR radiance
Background check information added in Bgckalt	
014213	Estimated cloud top height by CO_2-slicing
014214	Error on estimated cloud top height by CO_2-slicing
014215	Estimated cloud fraction by CO_2-slicing
014216	Error on estimated cloud fraction by CO_2-slicing
014217	Equivalent height from window channel
014218	Retrieved skin temperature from window channel
014219	Number of valid estimate (CO_2-slicing)
014220	Model air temperature, eta=1
014221	Surface model temperature
013214	Specific humidity at surface
059182	Surface model pressure